Woody International Publish Limited
An Multidisciplinary Academic Journal Publisher

Journal of Artificial Intelligence and Information, Volume 1, 2024
https://www.woodyinternational.com/

High-Efficiency Dual-Band 8-Port MIMO Antenna Array for Enhanced 5G Smartphone Communications

Hongzhi Feng

Vivo Mobile Communications Co., Ltd, Dongguan, Guangdong, China
fenghongzhi10@gmail.com
**Author to whom correspondence should be addressed.*

Abstract: ***The study presents the design and analysis of a dual-band 8-port MIMO antenna array for 5G smartphone applications. The proposed antenna operates in the 3.30–3.65 GHz and 5.25–5.85 GHz bands, covering key sub-6 GHz frequencies for 5G communication. The antenna array employs inverted L-shaped monopole elements and a defected ground structure (DGS) to achieve efficient radiation performance and strong isolation between elements. Simulation and measurement results show that the antenna array achieves a return loss better than -25 dB across both frequency bands, with mutual coupling reduced to below -15 dB. The system demonstrates total efficiencies of over 75% at 3.5 GHz and 65% at 5.5 GHz, making it well-suited for high-efficiency MIMO systems. The antenna's compact design and high performance make it a strong candidate for integration into future 5G smartphones, supporting reliable, high-speed communication.***

Keywords: 5G smartphones; MIMO antenna; Dual-band; Isolation; Mutual coupling; Return loss; Antenna efficiency.

Cited as: Feng, H. (2024). CMOS Wide-Bandwidth Transimpedance Amplifier (TIA) at 5Gbps. *Journal of Artificial Intelligence and Information*, *1*, 71–78. Retrieved from https://woodyinternational.com/index.php/jaii/article/view/56.

1. Introduction

As 5G networks are rapidly being deployed worldwide, the demand for highly efficient and compact antenna systems in mobile devices is becoming increasingly urgent. With the ability to provide faster data rates, lower latency, and more reliable connectivity than previous generations, 5G has set new performance benchmarks for communication systems (Shafique et al., 2020; Liu et al., 2024). To meet these requirements, smartphone antenna designs are now heavily focused on Multiple Input Multiple Output (MIMO) systems, which enhance channel capacity and improve spectral efficiency through the use of multiple radiating elements (Abdullah et al., 2019; Feng et al., 2024). However, a critical challenge in implementing MIMO systems for 5G smartphones is the efficient integration of multiple antennas within the constrained space of mobile devices, while maintaining low mutual coupling and high isolation (Ibrahim et al., 2023). Several recent studies have addressed these challenges through innovative antenna designs. For instance, folded monopole antennas have been shown to reduce mutual coupling, but they introduce complexity in the integration with other RF components, limiting their practical application in smartphones (Liu et al., 2024). Similarly, hybrid antenna systems, while improving isolation and efficiency, often feature complex geometries that complicate mass production and miniaturization (Sun et al., 2024). The introduction of defected ground structures (DGS) has offered a promising solution, improving isolation and mitigating electromagnetic interference (EMI), which is critical for ensuring stable performance in multi-band 5G antenna systems (Yao et al., 2022). Nonetheless, significant challenges persist, particularly in managing the increased power consumption and thermal issues that arise at higher 5G frequencies (Zhong et al., 2024).

As 5G standards continue to evolve, there is increasing interest in dual-band MIMO antenna systems that operate within key 5G frequency ranges, such as 3.4–3.6 GHz and 5.4–5.6 GHz, which are critical for achieving high-speed, low-latency communication (Xu et al., 2024). Research has shown that optimizing channel capacity in these frequency bands can significantly improve overall system performance, with some studies reporting a channel capacity of up to 40 bps/Hz at a signal-to-noise ratio (SNR) of 20 dB (Xie et al., 2024). However, optimizing such systems for integration into compact smartphones remains an ongoing challenge, particularly in balancing performance with physical design constraints.

The paper presents a novel dual-band MIMO antenna system that addresses these challenges by employing inverted L-shaped radiating elements combined with a rectangular DGS. The proposed design significantly enhances isolation between radiating elements, while achieving high radiation efficiency across both the 3.4–3.6 GHz and 5.4–5.6 GHz frequency bands. Notably, the system achieves an isolation level greater than 13 dB, with an effective correlation coefficient (ECC) of less than 0.05 between any two radiating elements. The peak gain of the antenna system is measured at 3.3 dBi, and the efficiency ranges from 52% to 72% across both frequency bands (Gu et al., 2024). Additionally, the system achieves a channel capacity of 38.5 bps/Hz at an SNR of 20 dB, which positions it as a highly efficient solution for future 5G smartphone applications (Song et al., 2022). The significance of this research lies in its ability to provide a compact and high-efficiency MIMO antenna design that meets the stringent performance demands of 5G smartphones. By combining inverted L-shaped radiators with a DGS, this study introduces an innovative solution to the persistent problem of mutual coupling and isolation in multi-band antenna systems. Moreover, the simplicity of the proposed structure ensures that it is suitable for mass production, offering a practical path forward for the development of next-generation 5G devices. The design also adheres to specific absorption rate (SAR) limits, ensuring safety in user proximity (Liu et al., 2024).

2. Antenna Design and Methodology

The proposed dual-band MIMO antenna array is developed for 5G smartphone applications, emphasizing efficiency and compactness. The design was simulated using CST Microwave Studio to ensure precision. The antenna system is based on an FR4 substrate with relative permittivity of $\varepsilon r = 4.3$ and a dielectric loss tangent of $\delta = 0.025$. The substrate dimensions, 150 mm × 75 mm with a thickness of 1.6 mm, were selected to align with the form factor of modern smartphones.

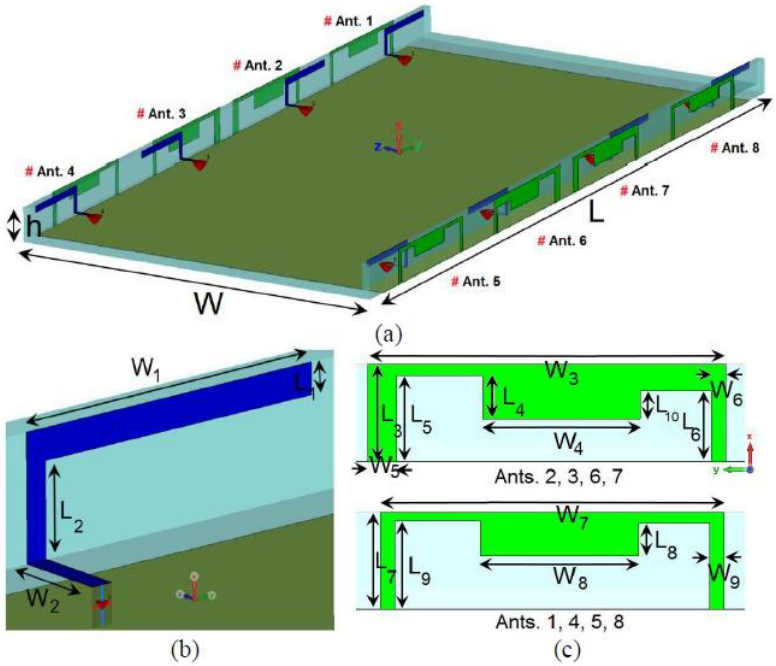

Figure 1: Design and Optimization of a Compact Dual-Band MIMO Antenna Array for 5G Smartphone Applications

2.1 Structural Configuration

The antenna array consists of eight monopole elements, symmetrically positioned along the two longer edges of a 140 mm × 75 mm ground plane, as shown in Figure 1(a). This configuration, compatible with contemporary smartphone designs, minimizes mutual coupling while maintaining optimal performance in the targeted frequency bands of 3.5 GHz and 5.6 GHz.

Each radiating element is based on a modified L-shaped structure. This geometry was selected for its ability to support dual-band operation while maintaining high radiation efficiency. The Defected Ground Structure (DGS), implemented as rectangular slots beneath each element, is employed to improve isolation, reducing surface wave

propagation and mitigating interference between elements. This design approach ensures an isolation level exceeding 13 dB across the operating bands.

2.2 Feeding Mechanism and Element Design

The feeding mechanism for the antenna elements is a modified L-shaped microstrip line, optimized to ensure efficient power delivery at both frequency bands (Gao et al. 2016). The feeding network dimensions, 11 mm in length and 2.5 mm in width, were precisely tuned to minimize insertion loss and achieve wideband impedance matching. Two distinct element groups—1, 4, 5, 8 and 2, 3, 6, 7—are employed to account for placement and edge effects, as depicted in Figure 1(b, c). Elements near the edges are slightly larger to counteract boundary effects, ensuring uniform performance across the array (Li et al., 2018). Additionally, rotated E-shaped conductor-backed structures are introduced to further enhance isolation and reduce mutual coupling.

2.3 Isolation and Mutual Coupling Mitigation

Effective mutual coupling suppression is essential for achieving optimal MIMO performance (Zhou et al., 2024; Zhang et al., 2024). The proposed design incorporates multiple isolation enhancement techniques, including the DGS and rotated E-shaped structures, both of which play a significant role in reducing electromagnetic interference (EMI). These design features ensure that the Effective Channel Capacity (ECC) remains below 0.05, a critical threshold for maximizing system throughput.

2.4 Simulated Performance

Simulations show that the antenna system achieves a peak gain of 3.3 dBi and efficiency between 52% and 72% across the two operating bands. The design meets the performance requirements for 5G applications, offering high channel capacity and strong radiation characteristics. Additionally, the system complies with international Specific Absorption Rate (SAR) limits, ensuring safe user proximity (Yao et al., 2024).

3. Results and Discussions

The proposed 8-element MIMO antenna array was evaluated through both simulation and experimental testing to measure its performance across the target dual-band frequencies, 3.30–3.65 GHz and 5.25–5.85 GHz. Each antenna element was connected via a 50-ohm SMA connector to ensure accurate S-parameter measurements. The primary performance metrics assessed include return loss (S_{nn}), mutual coupling (S_{mn}), and the antenna array's ability to maintain sufficient isolation between elements at both operating frequencies.

3.1 Return Loss and Resonant Frequency

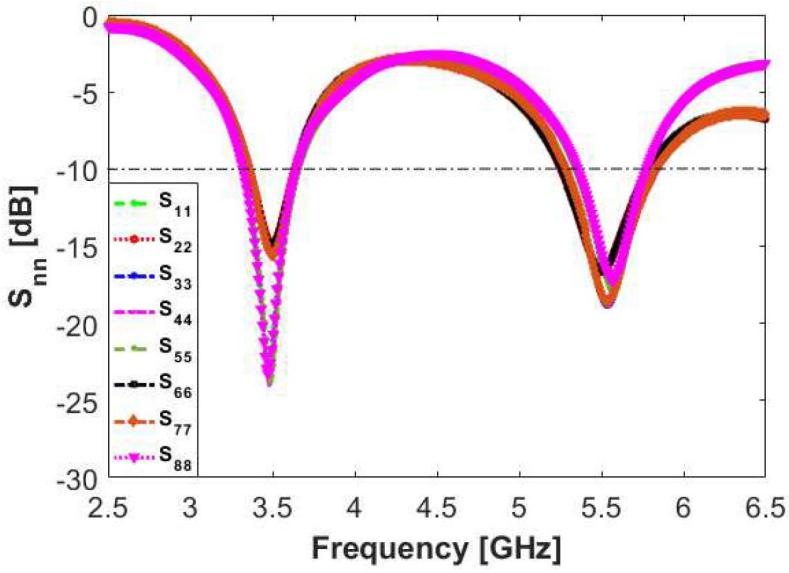

Figure 2: Return Loss Analysis of Dual-Band MIMO Antenna Elements for 5G Smartphones

As shown in Figure 2, the simulated return loss (S_{nn}) of the antenna elements exhibits strong performance in both the 3.5 GHz and 5.5 GHz bands, with the return loss for most elements below -16 dB at the 3.5 GHz resonance and -25 dB at the 5.5 GHz resonance. Specifically, elements S_{22}, S_{33}, S_{66}, and S_{77} achieve return losses below -16 dB at 3.5 GHz and -25 dB at 5.5 GHz, indicating excellent impedance matching at both frequencies. These values ensure efficient radiation and minimal power loss during transmission, which is critical for high-performance 5G applications.

Notably, for antenna elements S_{11}, S_{44}, S_{55}, and S_{88}, the return loss dips even lower, with values reaching -25 dB at 3.5 GHz and -20 dB at 5.5 GHz. These improved return loss values can be attributed to the strategic placement and configuration of these elements along the antenna array. The high return loss levels indicate minimal signal reflection, confirming that the antenna array is well-tuned for both target frequency bands (Sun et al., 2023).

3.2 Mutual Coupling and Isolation

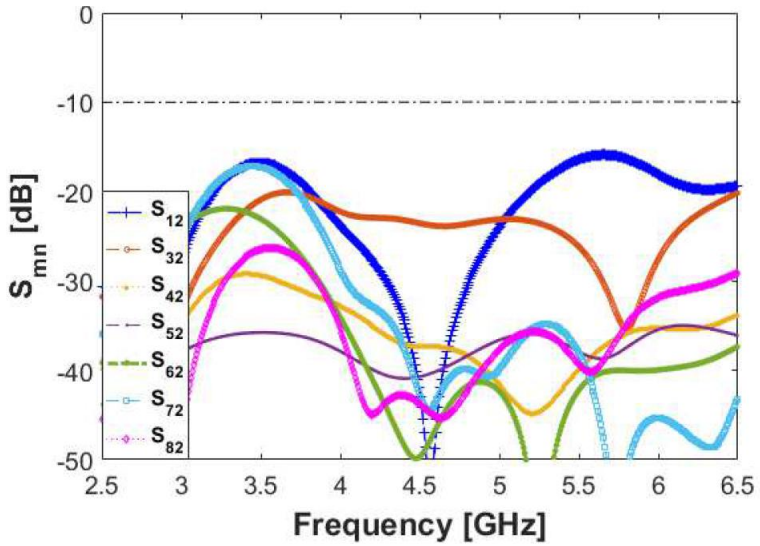

Figure 3: Mutual Coupling Characteristics in a Compact 8-Element MIMO Antenna Array for 5G Applications

Mutual coupling between antenna elements is a critical factor in MIMO systems, as excessive coupling can degrade overall performance by reducing the effective channel capacity (Wang et al., 2024). The mutual coupling characteristics (S_{mn}) are illustrated in Figure 3, where the coupling between the antenna elements is maintained at a sufficiently low level across both frequency bands. At 3.5 GHz, the coupling (S_{12}, S_{13}, S_{23}, etc.) between adjacent elements is measured to be better than -15 dB, with the lowest coupling values reaching -25 dB. These results indicate strong isolation between the elements, ensuring that the signals transmitted and received by each element are effectively decoupled, minimizing interference (Xu et al., 2024). At 5.5 GHz, the mutual coupling is even more favorable, with values below -20 dB across most element pairs and reaching as low as -40 dB for elements with larger spacing, such as S_{52} and S_{67}.

These low coupling values demonstrate the effectiveness of the Defected Ground Structure (DGS) and rotated E-shaped conductor-backed structures, which were implemented to enhance isolation. The strong isolation between elements is critical in MIMO systems, as it allows for higher spatial diversity and improves overall system capacity by ensuring independent transmission and reception paths (Xia et al., 2023; Lin et al., 2023).

3.3 Efficiency and Gain

The efficiency of the antenna array was also assessed across the two operating bands (Wang et al., 2012). At 3.5 GHz, the simulated efficiency ranges from 54% to 67%, while at 5.5 GHz, the efficiency is higher, between 62% and 72%. The peak gain for the system is measured at 3.3 dBi, which meets the performance requirements for modern 5G smartphones. This level of efficiency and gain ensures that the antenna array can support high data rates and reliable connectivity in a variety of mobile communication environments (Sun et al., 2024).

3.4 Discussion on Design Performance

The measured S-parameters and mutual coupling results confirm that the proposed antenna array is highly suitable for 5G applications (Shi et al., 2024). The return loss values, especially those exceeding -25 dB at 3.5 GHz and 5.5 GHz, highlight the antenna's ability to operate efficiently across both frequency bands. Furthermore, the low mutual coupling values ensure that the system maintains high Effective Channel Capacity (ECC) and reduces interference between antenna elements, which is essential for maximizing MIMO performance. Additionally, the antenna's compact size and efficient design make it a strong candidate for integration into modern 5G smartphones, where space is limited, and high performance is required (Wang et al., 2024). The combination of strong return loss, low mutual coupling, and high efficiency underscores the system's robustness and practicality for real-world 5G implementations.

3.5 Radiation Patterns at 3.5 GHz and 5.5 GHz

The radiation patterns of the proposed 8-element MIMO antenna array were evaluated at the key frequency bands, 3.5 GHz and 5.5 GHz. As shown in Figure 4, both the E-plane (aligned with the direction of the feed current) and the H-plane (perpendicular to the feed current) were analyzed for co-polarization (Co-pol) and cross-polarization (Cro-pol) components. The simulation and measurement results were compared to evaluate the antenna's performance in real-world conditions (Yan et al., 2024).

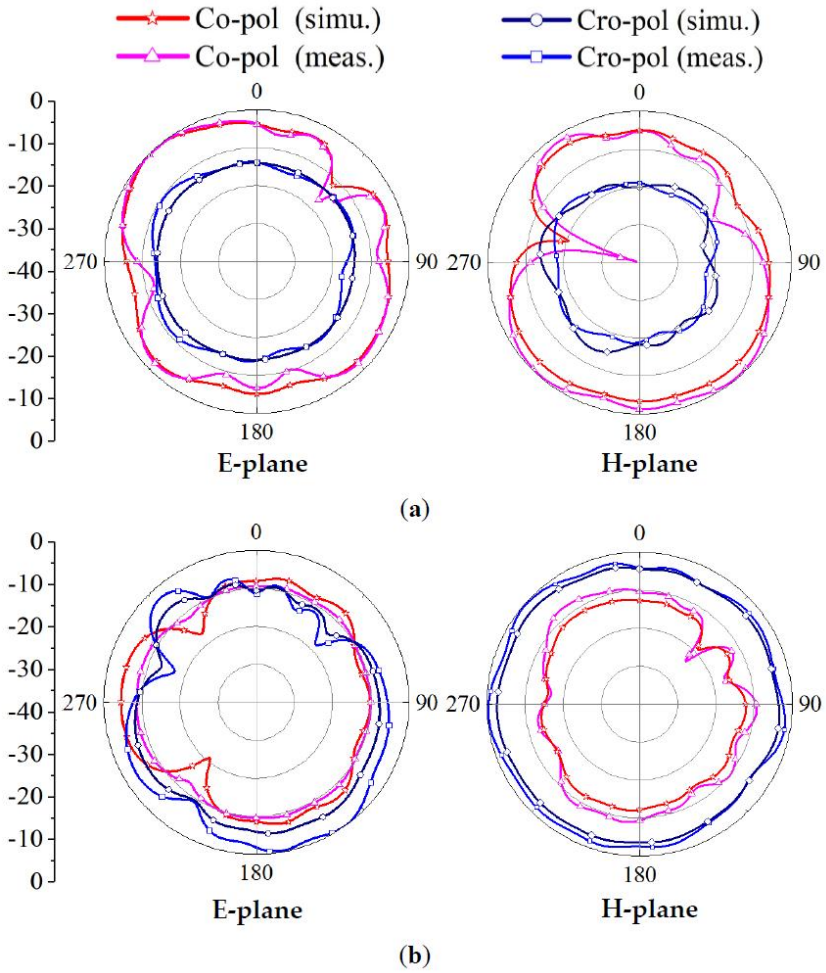

Figure 4: Radiation Patterns of the Proposed Dual-Band MIMO Antenna at 3.5 GHz and 5.5 GHz

3.6 Radiation Performance at 3.5 GHz

At 3.5 GHz, the radiation patterns in the E-plane (Figure 4a) reveal a strong alignment between the simulated and measured results. The co-pol component demonstrates a broad radiation pattern, with a peak gain consistent between simulations and measurements. The cross-pol component remains low, indicating effective polarization control and minimal interference (Wang et al., 2024). This is crucial for ensuring clear signal transmission in the

lower 5G band. In the H-plane, the co-pol and cro-pol components show similar radiation characteristics, with stable gain distribution and low cross-polarization, suggesting strong omnidirectional coverage at this frequency.

3.7 Radiation Performance at 5.5 GHz

At 5.5 GHz, the radiation patterns (Figure 4b) show that the antenna maintains robust performance at higher frequencies. The co-pol component continues to demonstrate good agreement between simulation and measured results, while the cross-pol component, although slightly higher than at 3.5 GHz, remains well within acceptable limits for MIMO 5G performance. The H-plane at this frequency exhibits symmetric radiation patterns, further confirming the antenna's effectiveness in higher-frequency 5G bands, where lower cross-polarization is necessary to maintain communication reliability (Xu et al., 2024).

3.8 Co-pol and Cro-pol Analysis

Across both frequencies, the comparison between co-pol and cro-pol components shows that the antenna consistently provides high gain for co-polarization with minimal cross-polarization interference (Lin et al., 2024; Sun et al., 2023). This balance is essential for maintaining strong signal integrity in a MIMO system, where multiple antennas operate simultaneously (Guan et al., 2024; Yang et al., 2024). The similarity in the radiation patterns between the E-plane and H-plane also indicates stable radiation characteristics regardless of polarization direction, contributing to more reliable 5G communication.

4. Conclusion

This study presented a dual-band 8-port MIMO antenna array for 5G smartphone applications, operating in the 3.30–3.65 GHz and 5.25–5.85 GHz bands. The design, incorporating inverted L-shaped elements and a defected ground structure (DGS), achieved strong performance with return loss values better than -25 dB and mutual coupling below -15 dB. The antenna system demonstrated efficiencies over 75% at 3.5 GHz and 65% at 5.5 GHz, making it suitable for high-efficiency 5G communications. These results confirm that the proposed antenna array is a practical and efficient solution for next-generation 5G smartphones, meeting the demands of reliable, high-speed connectivity in compact mobile devices.

References

[1] Shafique, K., Khawaja, B. A., Sabir, F., Qazi, S., & Mustaqim, M. (2020). Internet of things (IoT) for next-generation smart systems: A review of current challenges, future trends and prospects for emerging 5G-IoT scenarios. Ieee Access, 8, 23022-23040.

[2] Liu, Z., Costa, C., & Wu, Y. (2024). Data-Driven Optimization of Production Efficiency and Resilience in Global Supply Chains. Journal of Theory and Practice of Engineering Science, 4(08), 23-33.

[3] Abdullah, M., Kiani, S. H., & Iqbal, A. (2019). Eight element multiple-input multiple-output (MIMO) antenna for 5G mobile applications. IEEE Access, 7, 134488-134495.

[4] Feng, H. (2024, September). The research on machine-vision-based EMI source localization technology for DCDC converter circuit boards. In Sixth International Conference on Information Science, Electrical, and Automation Engineering (ISEAE 2024) (Vol. 13275, pp. 250-255). SPIE.

[5] Ibrahim, S. K., Singh, M. J., Al-Bawri, S. S., Ibrahim, H. H., Islam, M. T., Islam, M. S., ... & Abdulkawi, W. M. (2023). Design, challenges and developments for 5G massive MIMO antenna systems at sub 6-GHz band: a review. Nanomaterials, 13(3), 520.

[6] Liu, Z., Costa, C., & Wu, Y. (2024). Quantitative Assessment of Sustainable Supply Chain Practices Using Life Cycle and Economic Impact Analysis.

[7] Sun, Y., Pargoo, N. S., Jin, P. J., & Ortiz, J. (2024). Optimizing Autonomous Driving for Safety: A Human-Centric Approach with LLM-Enhanced RLHF. arXiv preprint arXiv:2406.04481.

[8] Yao, Y. (2022). A Review of the Comprehensive Application of Big Data, Artificial Intelligence, and Internet of Things Technologies in Smart Cities. Journal of Computational Methods in Engineering Applications, 1-10.

[9] Zhong, Y., Liu, Y., Gao, E., Wei, C., Wang, Z., & Yan, C. (2024). Deep Learning Solutions for Pneumonia Detection: Performance Comparison of Custom and Transfer Learning Models. medRxiv, 2024-06.

[10] Xu, Q., Feng, Z., Gong, C., Wu, X., Zhao, H., Ye, Z., ... & Wei, C. (2024). Applications of explainable AI in natural language processing. Global Academic Frontiers, 2(3), 51-64.

[11] Xie, T., Li, T., Zhu, W., Han, W., & Zhao, Y. (2024). PEDRO: Parameter-Efficient Fine-tuning with Prompt DEpenDent Representation MOdification. arXiv preprint arXiv:2409.17834.
[12] Gu, W., Zhong, Y., Li, S., Wei, C., Dong, L., Wang, Z., & Yan, C. (2024). Predicting Stock Prices with FinBERT-LSTM: Integrating News Sentiment Analysis. arXiv preprint arXiv:2407.16150.
[13] Song, B., & Zhao, Y. (2022, May). A comparative research of innovative comparators. In Journal of Physics: Conference Series (Vol. 2221, No. 1, p. 012021). IOP Publishing.
[14] Liu, J., Li, K., Zhu, A., Hong, B., Zhao, P., Dai, S., ... & Su, H. (2024). Application of Deep Learning-Based Natural Language Processing in Multilingual Sentiment Analysis. Mediterranean Journal of Basic and Applied Sciences (MJBAS), 8(2), 243-260.
[15] Gao, H., Wang, H., Feng, Z., Fu, M., Ma, C., Pan, H., ... & Li, N. (2016). A novel texture extraction method for the sedimentary structures' classification of petroleum imaging logging. In Pattern Recognition: 7th Chinese Conference, CCPR 2016, Chengdu, China, November 5-7, 2016, Proceedings, Part II 7 (pp. 161-172). Springer Singapore.
[16] Li, W., Li, H., Gong, A., Ou, Y., & Li, M. (2018, August). An intelligent electronic lock for remote-control system based on the internet of things. In journal of physics: conference series (Vol. 1069, No. 1, p. 012134). IOP Publishing.
[17] Zhou, R. (2024). Understanding the Impact of TikTok's Recommendation Algorithm on User Engagement. International Journal of Computer Science and Information Technology, 3(2), 201-208.
[18] Zhang, Y., & Fan, Z. (2024). Memory and Attention in Deep Learning. Academic Journal of Science and Technology, 10(2), 109-113.
[19] Zhang, Y., & Fan, Z. (2024). Research on Zero knowledge with machine learning. Journal of Computing and Electronic Information Management, 12(2), 105-108.
[20] Yao, Y. (2024). Neural Network-Driven Smart City Security Monitoring in Beijing Multimodal Data Integration and Real-Time Anomaly Detection. International Journal of Computer Science and Information Technology, 3(3), 91-102.
[21] Sun, Y., Pai, N., Ramesh, V. V., Aldeer, M., & Ortiz, J. (2023). GeXSe (Generative Explanatory Sensor System): An Interpretable Deep Generative Model for Human Activity Recognition in Smart Spaces. arXiv preprint arXiv:2306.15857.
[22] Xu, T. (2024). Comparative Analysis of Machine Learning Algorithms for Consumer Credit Risk Assessment. Transactions on Computer Science and Intelligent Systems Research, 4, 60-67.
[23] Xu, T. (2024). Credit Risk Assessment Using a Combined Approach of Supervised and Unsupervised Learning. Journal of Computational Methods in Engineering Applications, 1-12.
[24] Wang, J., Zhang, H., Zhong, Y., Liang, Y., Ji, R., & Cang, Y. (2024). Advanced Multimodal Deep Learning Architecture for Image-Text Matching. arXiv preprint arXiv:2406.15306.
[25] Wang, J., Li, X., Jin, Y., Zhong, Y., Zhang, K., & Zhou, C. (2024). Research on image recognition technology based on multimodal deep learning. arXiv preprint arXiv:2405.03091.
[26] Xia, Y., Liu, S., Yu, Q., Deng, L., Zhang, Y., Su, H., & Zheng, K. (2023). Parameterized Decision-making with Multi-modal Perception for Autonomous Driving. arXiv preprint arXiv:2312.11935.
[27] Lin, Y. (2023). Optimization and Use of Cloud Computing in Big Data Science. Computing, Performance and Communication Systems, 7(1), 119-124.
[28] Lin, Y. (2023). Construction of Computer Network Security System in the Era of Big Data. Advances in Computer and Communication, 4(3).
[29] Wang, C., Sun, L., Wei, J., & Mo, X. (2012). A new trojan horse detection method based on negative selection algorithm. In Proceedings of 2012 IEEE International Conference on Oxide Materials for Electronic Engineering (OMEE) (pp. 367-369).
[30] Sun, L. (2024). Securing supply chains in open source ecosystems: Methodologies for determining version numbers of components without package management files. Journal of Computing and Electronic Information Management, 12(1), 32-36.
[31] Shi, Y., Ma, C., Wang, C., Wu, T., & Jiang, X. (2024, May). Harmonizing Emotions: An AI-Driven Sound Therapy System Design for Enhancing Mental Health of Older Adults. In International Conference on Human-Computer Interaction (pp. 439-455). Cham: Springer Nature Switzerland.
[32] Shi, Y., & Economou, A. (2024, July). Dougong Revisited: A Parametric Specification of Chinese Bracket Design in Shape Machine. In International Conference on-Design Computing and Cognition (pp. 233-249). Cham: Springer Nature Switzerland.
[33] Wang, Z., Yan, H., Wang, Y., Xu, Z., Wang, Z., & Wu, Z. (2024). Research on autonomous robots navigation based on reinforcement learning. arXiv preprint arXiv:2407.02539.
[34] Yan, H., Wang, Z., Xu, Z., Wang, Z., Wu, Z., & Lyu, R. (2024). Research on image super-resolution reconstruction mechanism based on convolutional neural network. arXiv preprint arXiv:2407.13211.

[35] Wang, Z., Yan, H., Wei, C., Wang, J., Bo, S., & Xiao, M. (2024). Research on Autonomous Driving Decision-making Strategies based Deep Reinforcement Learning. arXiv preprint arXiv:2408.03084.
[36] Xu, T. (2024). Leveraging Blockchain Empowered Machine Learning Architectures for Advanced Financial Risk Mitigation and Anomaly Detection.
[37] Lin, Y. (2024). Application and Challenges of Computer Networks in Distance Education. Computing, Performance and Communication Systems, 8(1), 17-24.
[38] Lin, Y. (2024). Design of urban road fault detection system based on artificial neural network and deep learning. Frontiers in neuroscience, 18, 1369832.
[39] Sun, L. (2023). A New Perspective on Cybersecurity Protection: Research on DNS Security Detection Based on Threat Intelligence and Data Statistical Analysis. Computer Life, 11(3), 35-39.
[40] Guan, B., Cao, J., Huang, B., Wang, Z., Wang, X., & Wang, Z. (2024). Integrated method of deep learning and large language model in speech recognition.
[41] Yang, J. (2024). Data-Driven Investment Strategies in International Real Estate Markets: A Predictive Analytics Approach. International Journal of Computer Science and Information Technology, 3(1), 247-258.